

Towards the Formal Verification of Optical Interconnects

Sanaz Khan Afshar, Osman Hasan, and Sofiène Tahar

Department of Electrical and Computer Engineering, Concordia University

1515 St. Catherine West, Montreal, Quebec, Canada H3G 2W1

Email: {s_khanaf,o_hasan,tahar}@ece.concordia.ca

Abstract—Optical solutions have been proposed for on-die interconnect utilizing the speed-of-light signal propagation and the large bandwidth of the waveguides. However, the inability to efficiently analyze photonic devices, which are continuous in nature, using traditional analysis approaches somewhat limits their applications. In this paper, we present the formalization of two of the most widely used structures in optical interconnect systems, i.e., the planar waveguide and Fabry-Pérot cavity, using a higher-order-logic theorem prover. The proposed formalization can be utilized to precisely analyze many fundamental components of an optical interconnect system.

I. INTRODUCTION

Electrical interconnects are the primary bottleneck for the development of high-performance and low-power consumption devices. To address this problem, optical interconnects have emerged as the most promising alternative [1]. The higher frequency, shorter wavelength, and larger photon energy of light waves allow faster, wider bandwidth and minimum crosstalk between signal transmission paths of optical interconnects compared to electrical counterparts. These factors result in less propagation delays and higher signal integrity for on-die applications and also provide extremely dense, high-bandwidth I/Os onto a chip [2].

Considering the importance of optical interconnects as an alternate to electrical counterparts and their expected extensive usage in all domains, there is a dire need of reliable analysis tools which are as accurate as possible. The most commonly used computer based techniques for optical system analysis are based on simulation and numerical methods. There is an extensive effort on optimizing and improving simulation based approaches, which accordingly results in specialized tools in optics, e.g., *Lumerical solutions* [3]. However, the inherent nature of numerical and simulation based methods fails to bring 100% accuracy in the analysis. The next approach in optical system analysis is symbolic computations. Computer algebra systems incorporate a wide variety of symbolic techniques for the manipulation of calculus problems. Based on these capabilities, they have been also tried in the area of optical system analysis, which resulted in dedicated optical analysis packages, e.g., *Optica* [4]. However, the analysis results from computer algebra systems are also not 100% precise due to the many approximations and heuristics used for automation and reducing memory constraints.

Recently, formal methods have been employed for verification of optical systems, e.g., [5], [6], [7]. The main idea behind formal methods is to develop a mathematical model for the given system and analyze this model using computer-based

mathematical reasoning, which in turn increases the chances for catching subtle but critical design errors that are often ignored by traditional techniques, i.e., simulations and symbolic computations. Analyzing optical interconnects in nano-scales applications is done in electromagnetic optics. However, the reported formal analysis of optics are majorly focused on either ray optics [7] or quantum optics [6]. To the best of our knowledge, the only formalization done in electromagnetic optics is [5], which presents the formal analysis of planar waveguides using the higher-order-logic theorem prover HOL.

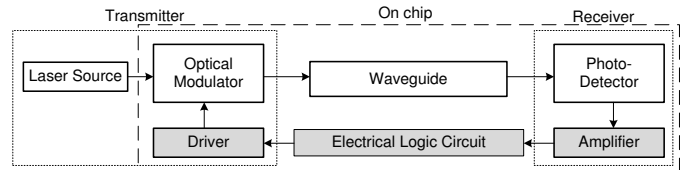


Fig. 1. Optical Interconnect System.

Figure 1 illustrates the schematic of an optical interconnect in an integrated photonics systems. In order to formally describe the behaviour of optical interconnects, all components and their interactions need to be formalized. We propose to employ higher-order-logic theorem proving for the formal verification of optical interconnects. This paper focuses primarily on two most fundamental components of interconnects, i.e., the waveguide and Fabry-Pérot cavity [8]. Physically, the waveguide can be described as an optical structure with three different refractive indices that allow the confinement of electromagnetic light waves within their boundaries by *total internal reflection* (TIR). Whereas, the Fabry-Pérot cavity, used extensively in on-die optical interconnects to improve their performance, is basically composed of two parallel flat mirrors that are closely spaced and illuminated near normal incidence. Light wave reflection between two mirrors leads to constructive and destructive interference of light fields resulting in a series of stationary electromagnetic waves in the cavity with interesting features. Depending on the application in which Fabry-Pérot cavity is used, the electromagnetic field of the light trapped within the cavity or the intensity of the light which is transmitted through the cavity are of high importance.

This paper presents a formal specification of the planar waveguide structure and the Fabry-Pérot cavity and based on these specifications, we formally verify a few key properties, which play a vital role in analyzing optical interconnect systems. The work described in this paper is done using the HOL Light theorem prover [9]. This choice was made because of the comprehensive theories of complex analysis [10] available in the HOL Light library.

The rest of the paper is organized as follows: Section II is about the formalization of the planar waveguide. Section III provides the formalization of Fabry-Pérot cavity and its application in lasers and photodetectors. Finally, Section IV concludes the paper.

II. PLANAR WAVEGUIDES

The planar waveguide, shown in Figure 2, is considered to be infinite in extent in two dimensions, let's say the yz plane, but finite in the x direction. It consists of a thin dielectric film surrounded by materials of different refractive indices. The refractive index of a medium is usually defined as the ratio between the phase velocity of the light wave in a reference medium to the phase velocity in the medium itself and is a widely used characteristic for optical devices. In Figure 2, n_c , n_s , and n_f represent the refractive indices of the cover region, the substrate region, and the film, which is assumed to be of thickness h , respectively.

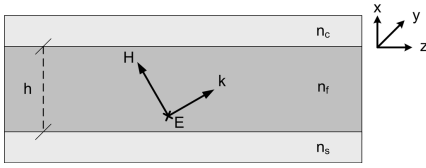


Fig. 2. Planar Waveguide Structure

The most important concept in optical waveguides is that of TIR. When a wave crosses a boundary between materials with different refractive indices, it is partially refracted and partially reflected. TIR happens when the refraction is minimum. In ray optics, this minimum is approximated to zero, however, in electromagnetic optics, it is modelled as an evanescent wave. Since, the objective of waveguides is to have minimum loss, we want to ensure TIR. This happens when the following two conditions are satisfied. Firstly, the refractive index of the transmitting medium must be greater than its surroundings, and secondly, the angle of incidence of the wave at the medium is greater than a particular angle, which is called *critical angle*. The first condition is satisfied by choosing n_f to be greater than both n_s and n_c . The second condition, on the other hand, depends on the angle of incidence of the wave on the boundary of the waveguide and thus involves the characteristics of the wave itself, which makes it more challenging to ensure.

In electromagnetic optics, propagation of light waves through a medium is characterized by their electromagnetic fields. Based on Maxwell equations [11], which completely describe the behaviour of light waves, it is not necessary to solve electromagnetic problems for each and every field component. It is well known that for a planar waveguide, it suffices to consider two possible electric field polarizations, *transverse electric* (TE) or *transverse magnetic* (TM) [8]. In this paper, we focus on the TE mode, though the TM mode can also be analyzed in a similar way. The electric and magnetic field amplitudes in the TE mode for the three regions of the planar waveguide are given as follows [8]:

$$E_y(x) = \begin{cases} Ae^{-\gamma_c x} & x > 0 \\ B \cos(\kappa_f x) + C \sin(\kappa_f x) & -h < x < 0 \\ De^{\gamma_s(x+h)} & x < -h \end{cases} \quad (1)$$

$$\gamma_c, \gamma_s, \kappa_f = \sqrt{\beta^2 - k_0^2 n_c^2}, \sqrt{\beta^2 - k_0^2 n_s^2}, \sqrt{k_0^2 n_f^2 - \beta^2} \quad (2)$$

$$H_z = \frac{j}{\omega \mu_0} \frac{\partial E_y}{\partial x} \quad (3)$$

where A , B , C , and D are amplitude coefficients, γ_c and γ_s are *attenuation coefficients* of the cover and substrate, respectively, κ_f is the *transverse component* of the wavevector $k = \frac{2\pi}{\lambda}$ in the guiding film, ω is the angular frequency of light and μ is the permeability of the medium. k_0 is the vacuum wavevector, such that $k_0 = \frac{k}{n}$ with n being the refractive index of the medium, and β and κ are the longitudinal and transverse components of the wavevector k , respectively, inside the film. The angle θ , is the required angle of incidence of the wave.

We formalized the electric and magnetic field equation, given in Equations 1 and 3, by utilizing the higher-order-logic formalizations of the Heaviside step function, derivative of a real-valued function and transcendental functions. We also formally verified the following expression for the magnetic field by differentiating the electric field expression.

$$H_z(x) = \frac{j}{\omega \mu_0} \begin{cases} -\gamma_c A e^{-\gamma_c x} & x > 0 \\ \kappa_f (-B \sin(\kappa_f x) + C \cos(\kappa_f x)) & -h < x \\ \gamma_s D e^{\gamma_s(x+h)} & x < -h \end{cases} \quad (4)$$

This completes the formalization of the light wave in a planar waveguide, which leads us back to the original question of finding the angle of incidence θ of the wave to ensure TIR. β is the most interesting vector in this regard. It summarizes two important characteristics of a wave in a medium. Firstly, because it is the longitudinal component of the wavevector, β contains the information about the wavelength of the wave. Secondly, it contains the propagation direction of the wave within the medium, which consequently gives us the angle of incidence θ . Now, in order to ensure the second condition for TIR, we need to find the corresponding β s. These specific values of β s are called the *eigenvalue of waveguides* since they contain all the information required to describe the behaviour of the wave and the waveguide.

The electric and magnetic field equations can be utilized along with their well-known continuous nature [8] in HOL-Light to verify the following useful relationship, which is usually termed as the *eigenvalue equation* for β .

$$\tan(h\kappa_f) = \frac{\gamma_c + \gamma_s}{\kappa_f \left(1 - \frac{\gamma_c \gamma_s}{\kappa_f^2}\right)} \quad (5)$$

The above relationship was verified under the assumptions that $(0 < h) \wedge (\beta < k_0 n_f) \wedge (k_0 n_s < \beta) \wedge (k_0 n_c < \beta) \wedge (0 < \omega) \wedge (0 < \mu_0) \wedge \neg(\kappa_f^2 = \gamma_c \gamma_s)$. The good thing about this relationship is that it contains β along with all the physical characteristics of the planar waveguide, such as refractive indices and height. Thus, it can be used to evaluate the value of β in terms of the planar waveguide parameters. This way, we can tune these parameters in such a way that an appropriate value of β is attained that satisfies the second condition for TIR, i.e., $\sin^{-1}\left(\frac{\lambda\beta}{2\pi}\right) < \text{critical_angle}$. All the values of β that satisfy the above conditions are usually termed as the TE modes in the planar waveguide.

Due to the inherent soundness of theorem proving, our verification results exactly matched the paper-and-pencil analysis counterparts for the eigenvalue equation, as conducted in [8], and thus can be termed as 100% precise. Interestingly, the assumption $\neg(\kappa_f^2 = \gamma_c \gamma_s)$, without which the eigenvalues are undefined, was found to be missing in [8]. This clearly demonstrates the strength of formal methods based analysis as it allowed us to highlight this corner case, which if ignored could lead to the invalidation of the whole analysis.

III. FABRY-PÉROT CAVITY

A Fabry-Pérot cavity, shown in Figure 3, consists of two parallel partially reflecting mirrors with a free space between them. Due to the effects of interference, only certain frequencies are sustained while others are suppressed by destructive interference. The two mirrors have field reflection coefficients of $r_1 e^{-jp_1}$ and $r_2 e^{-jp_2}$. These factors describe how much light is reflected by the front and back mirrors, M_f and M_b , respectively. r_1 and r_2 are the amplitude reflectivities of the two mirrors, respectively, and represent the ratio of transmitted electromagnetic field of light to the incident one, and p_1 and p_2 denote phase-shifts due to light penetration into the mirrors. The transmission coefficients of mirrors, t_1 and t_2 , describe how much light passes through each mirror. The two mirrors are separated by an l -width medium with absorption coefficient a , which measures the rate of decrease in the intensity of light as it passes through the cavity.

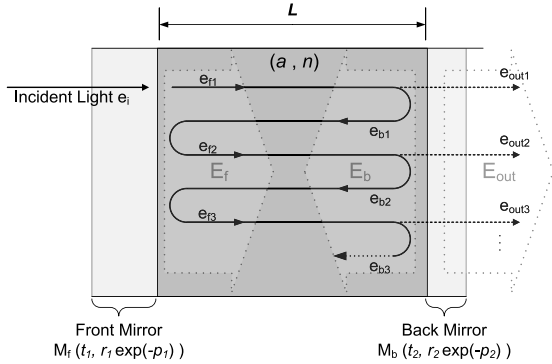


Fig. 3. Fabry-Pérot Cavity

The most important concept in Fabry-Pérot cavity is that of constructive interference of the light fields. The incident light, which is defined by electrical field E_i , is partially transmitted and partially reflected at each mirror. The amplitude of each subsequent reflection and transmission is reduced due to the losses encountered from previous reflection and the absorption of the medium, and an additional phase-shift of $2kl$ is introduced, for each round-trip they travel, whereas k is called wavevector and defined as $2\pi/\lambda$. In the Fabry-Pérot cavity the electrical field at three wavefronts is of high interest. Wavefronts are surfaces of constant electrical field phase. The first wavefront is located exactly at the output of cavity, which is the external surface of M_b . In Figure 3, this wavefront is represented by its corresponding electrical field E_{out} . The second wavefront is at the internal surface of M_f , represented by E_f , and the last one is at the internal surface of M_b , represented by E_b in Figure 3. Depending on the particular application, E_{out} , E_f , E_b or all can be of high importance. For applications, such as light emitting diodes,

lasers, and modulators, where the output of the system is in the form of optical signals, E_{out} is of high interest. On the other hand, E_f and E_b are of high interest when the system operates on optical signals, like photo-detectors.

We formalized the behaviour of Fabry-Pérot cavity in higher-order logic by first formalizing the behaviour of its two most basic components, i.e., a mirror and a medium. The behaviour of a mirror can be best described by Fresnel's law [8], according to which both reflection and refraction of light occur when a light strikes a surface with a different refractive index. The fraction of light that is reflected from the surface depends on its field reflection coefficient re^{-jp} and the refracted portion of light from the surface depends on its transmission coefficient t . These coefficients in turn depend on the refractive indices of the surface as well as the medium through which the light was traveling before striking the surface, the angle of incidence of light, and the characteristics of the light wave involved [8]. The second major component of the Fabry-Pérot cavity is the medium between the two mirrors. Firstly, some of the light is absorbed while passing through a medium and this absorption is characterized by the absorption coefficient a and the length of the medium l . Secondly, the phase of the light passing through a medium also changes based on the wavevector k and the medium length l .

Building on these basic definitions, we formalized the complete Fabry-Pérot cavity and verified relations for the electric fields at the internal and external surfaces of the two mirrors. These relations are then used to verify the intensity of light at the output of a cavity [8], formalized as follows:

$$I_o = \frac{(t_1^2 t_2^2 e^{-a l}) I_i}{(1 - r_1 r_2 e^{-a l})^2 \left(1 + \frac{4 r_1 r_2 e^{-a l}}{(1 - r_1 r_2 e^{-a l})^2} \sin^2(kl + \frac{p_1 + p_2}{2})\right)} \quad (6)$$

where I_i is the intensity of incident light at M_f . The above relationship was formally verified under the assumptions that $0 \leq r_1 \wedge 0 \leq r_2 \wedge r_1 < 1 \wedge r_2 < 1$. The formalization and verification details can be found in [12]. Equation 6 plays a vital role in formally reasoning about resonant cavity enhanced light-emitting diodes, lasers, and modulators. It allows to evaluate the transmission intensity for the Fabry-Pérot cavity in terms of the characterizing parameters of the system, i.e., r_1 , r_2 , p_1 , p_2 , t_1 , t_2 , a , and l and the light, i.e., the wavevector k . Therefore its formal verification allows us to precisely design many systems that utilize the transmission intensity of the Fabry-Pérot cavity.

Next, we analyze the interference of light inside the Fabry-Pérot cavity by building upon the formally verified electrical field relations at the internal surfaces of the mirrors, E_f and E_b , in presence of an active layer within the cavity, demonstrated in Figure 4. The interference behaviour is then utilized to formalize the ratio of the power absorbed by the active layer to the incident power, called quantum efficiency. Quantum efficiency is widely used in analyzing resonant cavity enhanced optical devices [13]. The expression is formalized as follows:

$$\eta = \frac{t_1^2 (e^{-a l_1} + r_2^2 e^{-a l_2} e^{-X}) (1 - e^{-a_d d})}{1 - 2 r_1 r_2 e^{-X} \cos(2kl + p_1 + p_2) + (r_1 r_2)^2 e^{-2(X)}} \quad (7)$$

where the variable X denotes the term $a l_1 + a l_2 + a_d d$. A simplified and widely used alternate expression for the

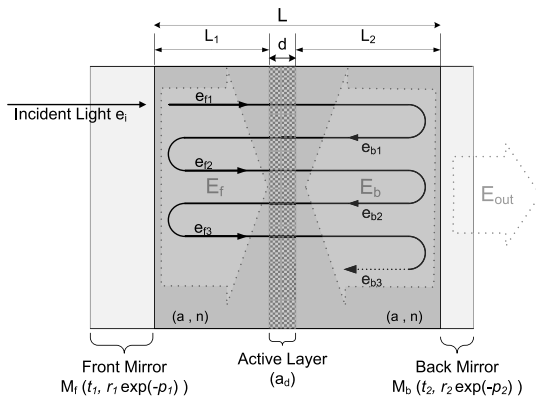


Fig. 4. Fabry-Pérot cavity with an Extra Active Layer

quantum efficiency can be obtained by assuming that the absorption of the layers on both sides of the active layer is negligible, i.e., $a = 0$. It is important to note here that since $k = \frac{2n\pi}{\lambda_0}$, where n is the refractive index and λ_0 is the vacuum wavelength of the incident light, it can be clearly observed from Equation 7 that the quantum efficiency is a periodic function of the inverse wavelength. Thus, by controlling the Fabry-Pérot cavity parameters (r_1, r_2, a_d), we can maximize the quantum efficiency of the cavity, for any particular light wavelength. Hence, the formal verification of Equation 7 plays a major role in the precise design of optical interconnects and other Fabry-Pérot cavity applications. Details on our formalization can be found in [12].

We now apply the above formal analysis of the Fabry-Pérot cavity on a laser output [14] and on quantum efficiency of a photodetector [13] as fundamental components of the optical interconnect. Details can be found in [12].

1) *Laser Source*: A symmetric Fabry-Pérot cavity, with $t_1 = t_2 = \sqrt{0.1}$, $r_1 = r_2 = \sqrt{0.9}$, no phase-shifts, i.e. $p_1 = p_2 = 0$, and $e^{-al} = 0.98$, illuminated by a gas-laser, has been studied by [14]. It is shown that for a selective range of wavelengths, over 70% of light intensity is transmitted through the cavity. The cavity has 0.6cm width and the laser wavelength is $\lambda_0 = 638.8nm$ which has $\Delta\lambda = 40nm$. This means k belongs to $[\frac{2\pi}{\lambda_0 + \Delta\lambda}, \frac{2\pi}{\lambda_0 - \Delta\lambda}]$. We utilized the formally verified Equation 6 to prove that the cavity, specified by the above parameters, has 70% transparency on intensity of light.

2) *Photodetector*: In [13], a conventional photodetector is compared to a photodetector enhanced by Fabry-Pérot cavity. A conventional photodetector, to have quantum efficiency over 90%, requires a very thick absorption layer in excess of $5\mu m$ while a Fabry-Pérot cavity with $r_1^2 = 0.9$, $r_2^2 = 0.99$, $a_d = 10^4 cm^{-1}$, $a \approx 0$, and $l_1 = l_2 = 1\mu m$, can remain within the same range of quantum efficiency with an $1\mu m$ -width absorption. In this cavity, phase-shifts and attenuation coefficients are considered to be zero, and $r_1^2 + t_1^2 = 1$. We utilized the Quantum Efficiency theorem, given in Equation 7, to formally verify in the HOL Light theorem prover that this photodetector has over 90% quantum efficiency.

The above formal analysis is straightforward which clearly demonstrates the effectiveness of our results in Section III. It is mainly due to the availability of the formally verified Equations 6 and 7 that we are able to tackle this kind of verification problem with such a minimal effort, while providing 100% precision.

IV. CONCLUSIONS

This paper presents the formal analysis of the planar waveguide and Fabry-Pérot cavity using the HOL Light theorem prover. Since these two are most widely used components in an optical interconnect system, their formal analysis can be regarded as the first step towards the formal analysis of the complete optical interconnect system. Due to the formal nature of the analysis, the results produced from our work can be termed as 100% precise, something that cannot be achieved by any other existing analysis approach. This feature makes our approach very useful for analyzing optical interconnect systems that are used in chips for safety-critical applications like medicine, military and transportation.

The successful analysis of planar waveguides and the Fabry-Pérot cavity clearly demonstrates the effectiveness and applicability of higher-order-logic theorem proving for analyzing optical interconnect systems. Some of the interesting future directions in this novel domain include the verification of the analysis of couplers that represent two or more optical devices linked together with an optical coupling relation, which can be done by building on top of the results presented in this paper.

ACKNOWLEDGEMENT

The authors would like to acknowledge the financial support from the Microelectronics Strategic Alliance of Quebec (ReSMIQ).

REFERENCES

- [1] The International Technology Roadmap for Semiconductors. www.itrs.net/, 2014.
- [2] M. Hauraylau, G. Chen, H. Chen, J. Zhang, N. A. Nelson, D. H. Albonesi, E. G. Friedman, and P. M. Fauchet. On-Chip Optical Interconnect Roadmap: Challenges and Critical Directions. *IEEE Journal of Quantum Electronics*, 12(6):1699–1705, 2006.
- [3] Lumerical solutions. www.lumerical.com/, 2014.
- [4] Optica. www.opticasoftware.com, 2014.
- [5] O. Hasan, S. Kh. Afshar, and S. Tahar. Formal Analysis of Optical Waveguides in HOL. In *Theorem Proving in Higher Order Logics*, volume 5674 of LNCS, pages 228–243. Springer, 2009.
- [6] M. Y. Mahmoud and S. Tahar. On the quantum formalization of coherent light in HOL. In *NASA Formal Methods*, volume 8430 of LNCS, pages 128–142. Springer, 2014.
- [7] U. Siddique, V. Aravantinos, and S. Tahar. On the Formal Analysis of Geometrical Optics in HOL. In *Automated Deduction in Geometry*, volume 7993 of LNCS, pages 161–180. Springer, 2013.
- [8] C.R. Pollock. *Fundamentals of Optoelectronics*. Tom Casson, 1995.
- [9] J. Harrison. HOL Light: A Tutorial Introduction. In *Formal Methods in Computer-Aided Design*, volume 1166 of LNCS, pages 265–269. Springer, 1996.
- [10] J. Harrison. Formalizing Basic Complex Analysis. In *From Insight to Proof: Festschrift in Honour of Andrzej Trybulec*, volume 10(23) of *Studies in Logic, Grammar and Rhetoric*, pages 151–165. University of Białystok, 2007.
- [11] J.D. Jackson. *Classical Electrodynamics*. John Wiley & Sons, Inc., 1998.
- [12] S. Kh. Afshar, O. Hasan, and S. Tahar. Formalization of Fabry Perot Resonator in HOL light. Technical Report, Concordia University, Montreal, Canada, 2013.
- [13] M. S. Ünlü and S. Strite. Resonant Cavity Enhanced Photonic Devices. *Journal of Applied Physics*, 78(2):607–639, 1995.
- [14] A. Yariv and P. Yeh. *Photonics: Optical Electronics in Modern Communications*, chapter 4, pages 160–164. Oxford University Press, 2006.